

Modification of the Photocatalytic Activity of Zinc Oxide by Doping Silver

Amjed M. Odeh¹, Ahmed S. Ferhod², Abbas J. Lafta^{*2}

¹Babylon University, College of Basic Education, Iraq

²Babylon University, College of Science, Iraq

Abstract: *The present study involves modification of zinc oxide by doping silver from an aqueous solution. Modification surface of zinc oxide was characterized by powder X-rays diffraction (PXRD), scanning electron microscopy (SEM), Fourier transform infrared spectroscopy (FTIR), energy dispersive X-rays spectroscopy (EDX) and UV-Visible fluorescence spectroscopy. Also the point zero charges (PZC) for neat and silver doped ZnO was investigated by potentiometric titration. From XRD patterns for neat and doped zinc oxide, doping zinc oxide in this level doesn't alter its crystallite. The photocatalytic activity of these materials was investigated by following photocatalytic degradation of dispersive red-50 and congo red dyes from their aqueous solutions. From this study it was found that doped zinc oxide showed a higher photocatalytic activity in comparison with the neat samples under the same reaction conditions.*

Keywords: zinc oxide, doped zinc oxide, congo red removal, photocatalytic removal of dyes

1. Introduction

In the recent years, and as a result of a massive technological and industrial development in all aspects of human life. Due to this large amount of industrial wastewaters are effluents into the surrounding environment. Examples of this are the textile industries, food industries, fertilizer industries, and paper industries¹⁻⁶. The disposal of large quantities of these wastes can cause high levels of environmental hazards. This arises from the fact that, these wastes normally contain appreciable amounts of the toxic organic compounds, and these can't be degraded easily by applying ordinary wastewater treatment methods such as adsorption, and biochemical methods^{7,8}. Due to this advanced oxidation processes (AOPS) seem to be as attractive alternative approaches for wastewater treatment⁹. The main concept of this approach is the formation of hydroxyl radicals which then contribute in the mineralization of wide range of toxic organic compounds that are present in these contaminated materials. In this context, AOPS can lead to fully mineralize these hazardous materials into friendly materials final products such as water, carbon dioxide and inorganic materials. These AOPS methods can be conducted by using heterogeneous photocatalysis semiconductors¹⁰⁻¹². Among different types of these photocatalytic semiconductors (SCS), zinc oxide (ZnO) is seemed to be as a good photocatalyst. This is due to its excellent physical and chemical properties such as non-toxicity, high reflective index, easily to synthesize, high photo-thermal stability and it can be reused easily. The main drawback with ZnO is its high bandgap energy (3.37 eV), this means that it can be excited only in UV region of the solar spectrum¹³. This makes ZnO is not active photocatalyst in the visible region of the spectrum and according to this it can't be applied for solar radiation photocatalytic processes. Generally, for the photocatalytic degradation processes, it was found that nano-sized ZnO is better than that of large size particles. This arises from microscopic properties of small particles materials (nano-scales) such as high surface area with high porosity of materials^{14,15}. This can lead to high ability of these materials

towards adsorption of reactants with high efficiency which gives high adsorption capacity and hence it can increase rate of the photocatalyzed reaction. Besides that, nano-sized materials have high quantum confinement which can enhance the rate for electron/hole transport from the bulk of the SC particles into the surface in order to contribute in redox- reactions on the surface. This process can reduce the rate of recombination reaction between (e^-/h^+) pairs which normally occurs in case of neat photocatalysts. The last process reduces the efficiency of the photocatalytic activity, so that many approaches have been undertaken to reduce the rate of recombination reaction^{16,17}.

One of these approaches is the doping of the SC with the metal particles. According to this method, metal particles act as a temporary sink for collection of electrons from the CB of the SC. This can increase the rate for charge separation and hence cause a significant reduction in back electron transfer in to the valence band of the semiconductor¹⁸⁻²⁰.

In the present study, modification of the photocatalytic activity of zinc oxide by doping silver was investigated. The photocatalytic activity for neat and silver doped zinc oxide was conducted by the following of the photocatalytic degradation of the dispersive red 50 and congo red dyes over neat and silver doped zinc oxide.

2. Experimental Part

2.1 Used Dye

Dispersive red -50 (DR50), its molecular formula ($C_{17}H_{16}ClN_5O_2$) and Congo red dye (CR), its molecular formula ($C_{32}H_{22}N_6Na_2O_6S_2$), the last dye is a sodium salt of a secondary diazo dye. These dyes were used as a model of polluted dyes in this study. Distilled water was used to prepare all the solutions and reagents in this work. These two dyes were used as a model for photocatalytic degradation in this study and they were used as provided without any further purification. Schematic description of these dyes is shown in Figure.1.

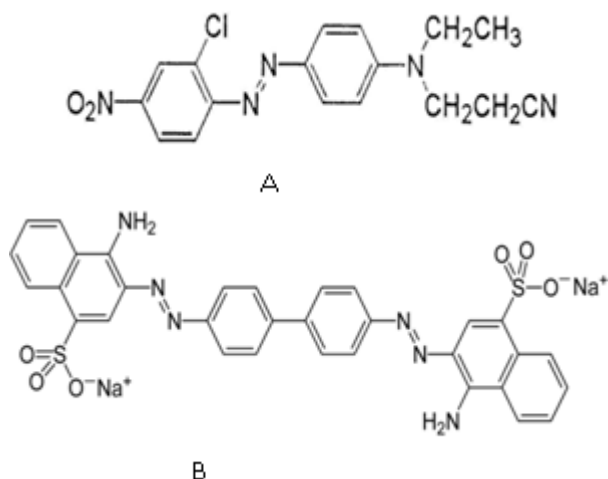


Figure 1. Molecular structure of dispersive red (A), and congo red (B)

2.2 Modification of Zinc oxide surface

Doping of silver on zinc oxide surface was conducted using 50 ml aqueous solution of 0.1 molar of silver nitrate (BDH, 99%) was irradiated with UV radiation using a Candle (5 watt.) with continuous stirring at 25 °C. This mixture was agitated for 30 min and the black colloidal of silver metal appeared and no silver ion precipitated as AgCl after irradiation. ZnO (Fluka company, 99.5%) 5 g was mixed with silver colloidal solution, this was stirring for 1 hour at 25 °C in air atmosphere, then the proposed precipitate of Ag/ZnO was filtrated off and washed with ethanol several times and then dried at 80-100 °C for overnight.

2.3 Point zero charges for neat and silver doped zinc oxide

The point zero charges of the neat and silver doped zinc oxide were calculated by potentiometric titration²¹. According to this method, 100 mL of 0.03 M KNO₃ was used as a blank solution and 1 mL of 1M NaOH was added. The resulted solution was titrated with HNO₃ (0.10M). A mixture of 100 mL of KNO₃ with 0.10 g of each of ZnO and Ag/ZnO was stirred for 24 hour. After that, 1.0 mL of NaOH was added and then titrated with HNO₃ using the same process that was following the blank solution. The results of the titration are plotted as a volume of the added acid (VS) pH of the mixture and the intersection point was taken to be equal to the PZC. These results are shown in Table 5.

2.4 Scanning electron microscopy (SEM)

The morphology of both neat and doped zinc oxide was investigated by using Scanning Electron Microscope Inspect 550, Netherland. SEM was operated at 25 kV and derided samples of AC were adhesive on carbon tape attached to aluminum – stubbed sputter coated with platinum.

2.5 Energy dispersion X-ray spectroscopy (EDX)

The concentration of silver in the samples of Ag/ZnO was investigated by using Energy dispersion X-ray (EDX), Bruker Nano GmbH, Germany.

2.6 Fourier transform infrared spectroscopy (FTIR)

FTIR spectra for bare ZnO and that doped with silver were recorded by using Perkin Elmer Spectrophotometer. Measurements were conducted in the wave numbers ranged from 450 to 4000 cm⁻¹. The samples were grounded with KBr at a ratio roughly 1/50 of all samples. Then, the mixed samples were made as pellets by using a suitable pressing with Perkin Elmer hydrolytic pump. All spectra were recorded in range of 450- 4000 cm⁻¹ with a resolution of 1 cm⁻¹ for each scan.

2.7 Fluorescence spectroscopy

Fluorescence spectra for each of ZnO and Ag/ZnO were recorded via suspended these materials in ethanol. Measurements were conducted by excitation of the samples at 300 nm at room temperature. Measurements were run using fluorescence spectrophotometer (Spectrofluorophotometer Shimadzu, RF- 5301PC.)

2.8 X-ray powder diffraction (PXRD)

Powder X-rays diffraction patterns for both neat and silver doped zinc oxide were recorded using Simadzu-6000 X-ray diffractometer with a nickel filter using monochromatized CuK α radiation at 40 kV and 30 mA was used throughout to detect the crystalline structure of the films. The films were scanned at 2° (2 θ) per min. and the scan range was 20° 2 θ to 60° 2 θ . The intensity was recorded with a chart speed of 25 mm/min.

2.9 Photocatalytic degradation of disperse red-50 and congo red

Photocatalytic activity for neat and silver doped zinc oxide was investigated by following photocatalytic fragmentation of DR50 dye and CR dye over a suspension of zinc oxide. In all experiments, 0.10 g of the used catalyst was added to 100 mL of 50 ppm of dye with stirring for ten minutes prior to irradiation to reach adsorption equilibrium under dark conditions. Then the slurry was irradiated with high pressure mercury lamp (high pressure mercury lamp (HPML), 125 watt. CG. Germany) with continuous stirring, periodically, samples (2 mL) of the reaction mixture was withdrawn and centrifuged carefully. To follow photodegradation of the dye under irradiation, the absorbance was measured to each dye at maximum wavelength 496 nm for congo red and 510 nm for dispers red.

3. Results and Discussion

3.1 Point zero charges for neat and silver doped zinc oxide

The point zero charges for zinc oxide and its doped form with Ag were investigated by using potentiometric titration using KNO₃ as a blank solution. The results are shown in Table 1.

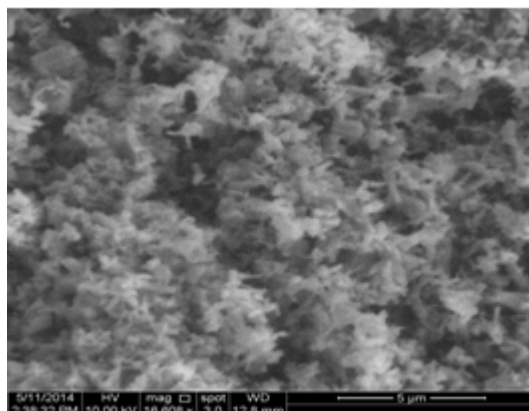
Table 1: The PZC values for neat and silver doped zinc oxide

Sample	Neat ZnO	Ag/Zno
PZC (pH)	9.15±0.12	9.32±0.10

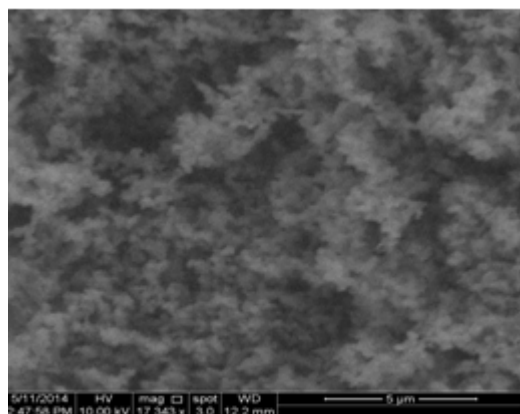
From these results it can be seen that the PZC for Ag doped zinc oxide was shifted towards relatively higher value of pH (more basic). This probably arises from the contribution of the adsorption of ions and /or some impurities on the surface of ZnO. These species can contribute in the slight change of the value of PZC for Ag/ZnO^{22,23}.

3.2 Scanning electron microscopy (SEM)

SEM images for neat and silver doped zinc oxide are represented in Figure 2. Neat powder of nanoparticle zinc oxide was homogeneous and relatively agglomerated with average particles size around (18 nm). This probably arises from the uniform distribution of zinc cation in three dimensional structure²⁴. The presence of agglomerates may result from densification that results due to the narrow space between particles. For Ag/ZnO, the sample turned more homogeneous with relatively larger particle size around (29 nm)²⁵



ZnO neat



Ag/ZnO

Figure 2: SEM images for neat and silver doped zinc oxide

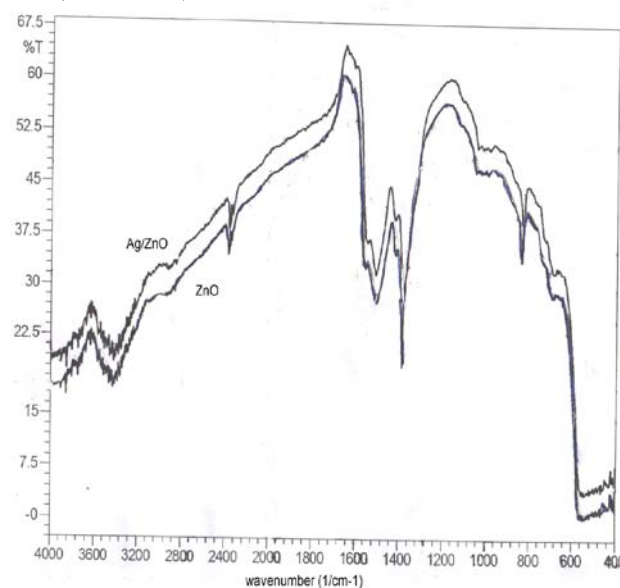
3.3 Energy dispersive x-ray patterns (EDX)

The chemical stoichiometry for ZnO and Ag/ZnO was followed by using EDX. Silver concentration in Ag/ZnO

sample was investigated by EDX technique, the concentration of silver dopant was around 4.58%. The results of EDAX analysis shows that 5% Ag dopant is present in the doped zinc oxide with silver. In this study it was aimed to dope of 4.58%, a slight decrease or increase probably arises from leaching out of unbound silver upon washing the crude sample prior to calcinations to yield final Ag/ZnO doped sample²⁶.

3.4 FTIR spectra for neat and Ag doped zinc oxide

FTIR spectra for samples of zinc oxide and that doped with silver are shown in Figure 3. The important feature of these spectra is that (shows the peak at 450 cm⁻¹ which is a distinct stretching vibration mode for zinc oxide i.e finger print for ZnO (Zn-O bond).

**Figure 3:** FTIR spectra for neat and silver doped zinc oxide

From this figure FTIR spectrum for silver doped zinc oxide is seemed to be similar to that for neat zinc oxide. According to these spectra, bands around 1630 cm⁻¹ and that around 3436 cm⁻¹ are assigned to the stretching modes of OH groups that are present in the catalyst. The bands around 450 and 590 cm⁻¹ are related to the bending vibration of the characteristic peak for Zn-O bonds. Generally, there were no further peaks upon doping silver, this indicates that doping silver was dispersed efficiently without formation any clusters of silver within zinc oxide structure²⁷. Absorption band around 3400 cm-1 is assigned to vibration mode of O-H group, and that appears around 2900 cm-1 can be assigned to C-H modes. The band that appears around 1400-1600 cm-1 are related to C=O stretching mode. Absorption band around 2350 cm-1 which may be resulted from the CO₂ adsorption on the surface. The characteristic band around 450 -550 cm-1 is related to Zn-O bonding in the semiconductor²⁸.

3.5 Fluorescence spectroscopies for neat and silver doped zinc oxide

Fluorescence spectra for neat and silver doped zinc oxide are shown in Figure 4. From these spectra it can be seen that there are two fluorescence emissions for these materials one of them appears in UV region of the spectrum around (300

nm). The other peaks appear in visible region around (420 nm). Fluorescence peak that appears at UV region can be attributed to the excitation luminescence of the bandgap of ZnO. The peaks that appear in the visible region are related to oxygen defects and interstitial zinc species that result by UV excitation²⁹⁻³¹.

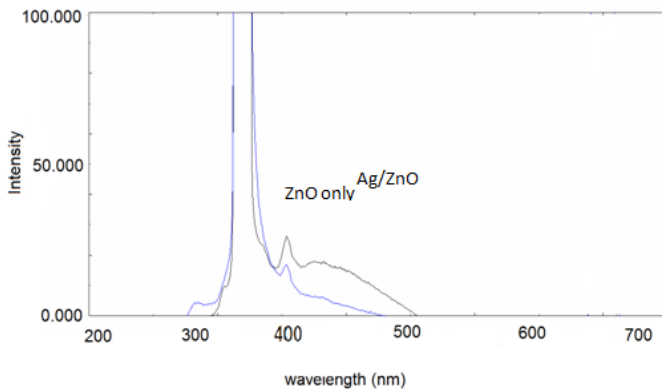


Figure 4: Fluorescence spectra for neat and silver doped zinc oxide

3.6 X-ray powder diffraction (PXRD)

The patterns of X-rays for neat and doped zinc oxide are shown in Figure 5. From this figure it is clear that doping silver on zinc oxide in this ratio (5%) doesn't alter its crystallite, almost the pattern that was recorded for Ag/ZnO is similar to that for neat zinc oxide.

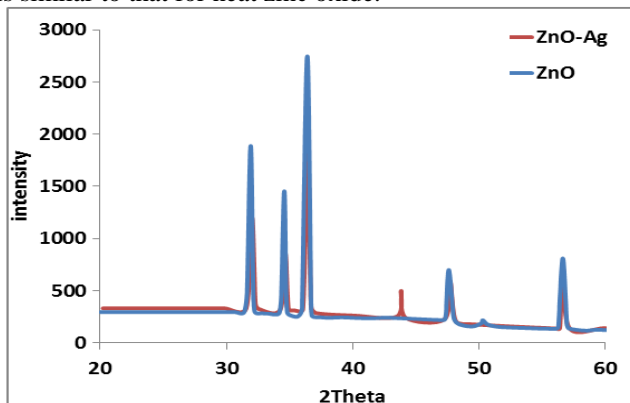


Figure 5: X-ray patterns for neat and silver doped zinc oxide

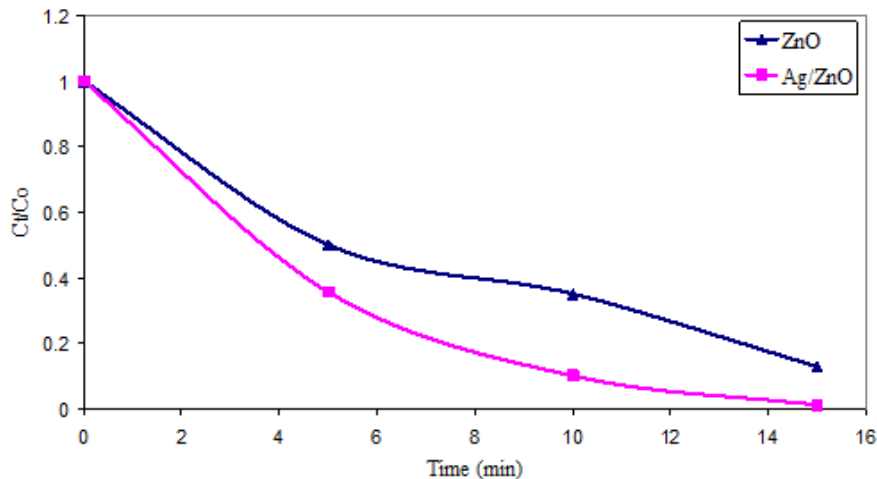


Figure 6: Degradation of dispersive red dye (50 ppm) over ZnO and Ag/ZnO at 28 °C using 0.10 g of the catalyst under ambient air atmosphere

There was a weak new peak that appears for doped zinc oxide around ($2\theta = 43^\circ$), also there was a very weak peak in ZnO pattern was disappeared in the pattern of doped zinc oxide. The peak around $2\theta = 43$ may be related to the presence of the metal on the surface of that semiconductor. However, for a transition metal like silver that has ionic radii much greater than that of zinc ion can't be introduced at ZnO lattice, instead of this Ag particles were homogeneously distributed within ZnO matrix as metallic silver particles. So that doping silver doesn't affect crystallite structure of zinc oxide³². Generally, the peaks of neat zinc oxide were boarder than that for the doped form, this indicates that it has smaller particle size in comparison with the doped form that has a thinner peaks which means it has relatively larger particle size. This observation was confirmed by applying Scherer equation³³ in the estimation of particle size which was 17.818 nm, and 29.106 nm for ZnO and Ag/ZnO respectively.

3.7 Photocatalytic activity for neat and silver doped zinc oxide

The photocatalytic degradation of pollutants in the wastewater to yield final fragmentations such as CO_2 , H_2O and some inorganic materials seems to be challenging goals in the development methods that are utilized in the removal of environmental pollutants. In this study, photocatalytic activity of these materials was investigated by following photocatalytic degradation of each of DR-50 and CR dyes over suspension of neat zinc oxide and that doped with silver. In all experiments, 0.10 g of materials was suspended in 100 mL of aqueous solution of the used dye 50 ppm. After performed of adsorption equilibrium, mixture was irradiated at 28 C with continues stirring. The degradation of dye was followed by measuring absorbance at 496 nm and 510 nm for RD-50 and CR dye respectively. The result were recorded as loss of optical intensity as a function of time for each dye for two cases using zinc oxide alone and using silver doped zinc oxide. These results are represented in Figures 6 and 7.

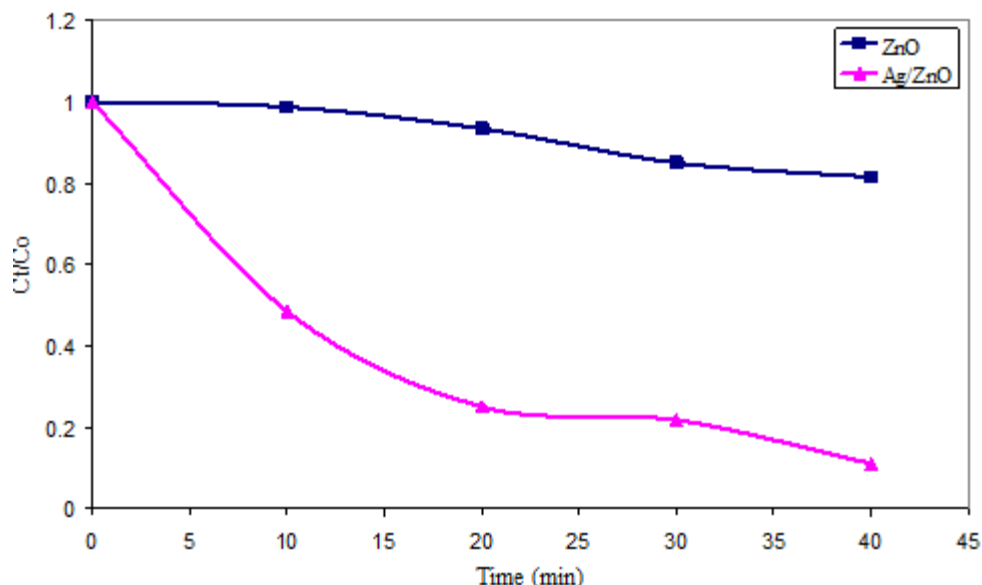


Figure 7: Degradation of congo red dye (50 ppm) over ZnO and Ag/ZnO at 28 °C using 0.10 g of the catalyst under ambient air atmosphere

From the above results, it can be seen that there was an enhancement in dispersive dye removal using silver doped zinc oxide in comparison to use neat zinc oxide as a photocatalyst. The percentage for dye removal was 98% and 85% for doped and neat oxide respectively. The results for congo red removal over a suspension of neat and silver doped zinc oxide was 19% and 79% respectively. For these two cases, it is clear that there was a considerable improvement in the photocatalytic activity for the doped form in terms of dye removal. This probably arises from the contribution of the metal particles in the capturing of conduction band electron by silver particles on the surface of semiconductor. It is believed that metal particles act as a sink for electron by formation an accepting level lower than that of CB of ZnO, this results in reduction the rate of recombination reaction which normally occurs between conduction band electron and valence band hole^{34,35}. By comparison removal percentage for these two dyes under the same reaction conditions, it can be found that dispersive red was removed effectively in short time in comparison with congo red at the same reaction parameters. This can be attributed to the diffusion limitation of this type of reaction as congo red is too large molecule in comparison with small size of the dispersive dye. Generally, in heterogeneous reactions diffusion limitation of the reaction reactants and products can lead to reduce the rate of photocatalyzed reaction significantly.

4. Conclusions

From the obtained results it was found that doping silver on zinc oxide in this ratio doesn't affect on its crystallite structure as it was found from its PXRD patterns that were almost similar to that obtained for non-doped zinc oxide. Also we found that doping silver on zinc oxide surface doesn't affect significantly on its PZC. The photocatalytic activity for doped samples was more efficient for neat samples. Also the photocatalytic removal of DR-50 dye was effectively higher than that for CR dye and this probably arises from diffusion limitation as the second dye is too bulky in comparison with the first one.

References

- [1] Shanthi M., and Kuzhalosai V., *India Journal of Chemistry*, 2012, **428**, 51.
- [2] J. Pignatello, Lui D., and Huston P., *Environ. Sci. Technol.*, 1999, **33**, 1832.
- [3] Arslan I., Balcioglu I., and Tukhanen T., *Chemosphere*, 1999, **39**, 2767..
- [4] Huston L., and Pinatello J., *Water Res.*, 1999, **33**, 1238.
- [5] Gary K., Amita M., Kumar R., and Gupta R., *Dyes and Pigments*, 2004, **63**, 243.
- [6] Appling G., and Lin C., *Chemosphere*, 2002, **46**, 561.
- [7] Latha G., and Shanthi M., *J. Theor. Exp. Biol.*, 2007, **4**, 51.
- [8] Perez M., Torrades F., and Domenech X., *J. Perol. Water Res.*, 2002, **36**, 526.
- [9] Dezhongyu, Ruzuicai and Zhihongliu, *Spectrochim. Acta. A*, 2004, **60**, 1617.
- [10] Attia A., Kadhim S., and Hussein F., *E. J. Chem.*, 2008, **5(2)**, 219.
- [11] Vino R., and Mudras G., *J. India Inst. Sci.*, 2010, **90**, 189.
- [12] Doug Z., Han B., Qian S., and Chen D., *J. of Nanomaterials*, 2012, **1155**, 2011.
- [13] Huang M., Mao S., and Feick H., *Science*, 2001, **292**, 1897.
- [14] Vayssieres L., *Advanced Materials*, 2003, **15**, 464.
- [15] Wei A., Xu C., Sun W., Huang W., and Lo G., *J. of Display Technology*, 2008, **4**, 9.
- [16] Szerok M., Song J., and Blackledge C., *Chemical Physics Letters*, 2005, **404**, 171.
- [17] Nakajima N., Kato H., Okazaki T., and Sakisaka Y., *Surf. Sci.*, 2004, **561**, 93.
- [18] Fijushima A., Rao N., and Tryk D., *J. Photochem. Photobiol. C: Photochem. Rev.*, 2000, **1**, 1.
- [19] Paola A., Marci G., Palmisano L., Schiavello M., Vosaki K., and Ikeda S., *J. Phys. Chem. B*, 2002, **106**, 637.
- [20] Connelly K., and Adriss H., *Green Chem.*, 2012, **14**, 260.

- [21] Vakros J., Kordulis C. and Lycourghiotis A., *Chem. Commun.*, 2002, **17**, 1980.
- [22] Noh J., and Schwary J., *J. Colloid Interface Sci.*, 1989, **130**, 157.
- [23] Paola A., Marci G., Palmisano L., Schiavello M., Uosaki K., Ikeda S., and Ohtani B., *J. Phys. Chem. B*, 2002, **106**, 637.
- [24] Yun W., Shin Y., and Cho S., *J. Kor. Ceram. Soc.*, 1998, **35(3)**, 498.
- [25] Ryu J., Lim C., and Auh K., *J. Kor. Ceram. Soc.*, 2002, **39(3)**, 321.
- [26] Narayanan B., Yaakob Z., Koodathil R., Chandralayam S., Sugunan S., Saidu F., Malayattil V., *European Journal of Scientific Research*, 2009, **28(4)**, 566.
- [27] Jun S., Kim S., Han J., *J. Kor. Ceram. Soc.*, 1998, **35(3)**, 209.
- [28] Taps A., Majewaski P., Aldinger F., *J. Am. Ceram. Soc.*, 2000, **83(12)**, 2954.
- [29] Li D., Leung Y., Djuricic A., Liu Z., Xie M., Shi S., Xu S., Chan W., *Appl. Phys. Lett.*, 2004, **85**, 1601.
- [30] Djuricic A., Choy W., Roy V., Leung V., Kwong C., Cheah K., Rao T., Chan W., Lui H., *Adv. Funct. Mater.* 2004, **14**, 856.
- [31] Xu P., Sun Y., Shi C., Xu F., Pan H., *Nucl. Instrum. Methods Phys. Res.*, 2003, **199**, 286.
- [32] Seery M., George R., Floris P., Pillai S., *J. Photochem. Photobiol. A: Chem.*, 2007, **189**, 258.
- [33] Dorofeev D., Streletskii A., Povstugar I., Protasov A., Elsukov E., *Colloid Journal*, 2012, **74(6)**, 675.
- [34] Rohmann C., Wang Y., Muhler M., Metson J., Idriss H., C. Wool C., *Chem. Phys. Lett.*, 2008, **460**, 10.
- [35] Mogyorosi K., Kmetyko A., Czirbus N., Vereb G., Sipos P., Dombi A., *React. Kinetic, Catal. Lett.*, 2009, **98**, 215.